



Evaluation of diatomaceous earth in the removal of crystal violet dye in solution

Grey C. Castellar-Ortega^{a*} • María M. Cely-Bautista^b • Beatriz M. Cardozo-Arrieta^a •
Javier E. Jaramillo-Colpas^c • Luis C. Moreno-Aldana^d • Jesús S. Valencia-Ríos^d

^aDepartamento de Ciencias Básicas, Facultad de Ingeniería, Universidad Autónoma del Caribe, Barranquilla, Colombia

^bFacultad de Ingeniería, Universidad del Atlántico, Barranquilla, Colombia

^cDepartamento de Ciencias Naturales y Exactas, Universidad de la Costa, Barranquilla, Colombia

^dLaboratorio de Catálisis Heterogénea, Aplicaciones Fisicoquímicas del Estado Sólido,
Departamento de Química, Facultad de Ciencias, Universidad Nacional de Colombia, Bogotá D.C., Colombia

Received 03 28 2021; accepted 11 16 2021

Available 08 31 2022

Abstract: In this research, the adsorption capacity of diatomaceous earth in the removal of the crystal violet dye (CV) in aqueous solution was evaluated. The experimental methodology began with the determination of the texture properties by adsorption-desorption isotherms with N₂ at 77 K, the identification of functional groups by Fourier transform infrared spectrophotometry (FTIR), morphology by scanning electron microscopy (SEM) and, the pH of the isoelectric point by the point of zero charge (PZC). A categorical multifactorial design was developed with factors such as the initial concentration of the dye, the temperature and the initial pH of the solution. The maximum adsorption capacity was of 96.1 mg/g up to 30°C and pH 8, satisfactorily fitting the experimental data to the Langmuir isotherm model, suggesting a monolayer adsorption mechanism on a homogeneous surface. In conclusion, diatomaceous earth can be considered as an efficient adsorbent in the removal of CV in aqueous solution.

Keywords: Diatomaceous earth, crystal violet, adsorption isotherms, adsorption capacity

*Corresponding author.

E-mail address: grey.castellar@uac.edu.co (Grey C. Castellar-Ortega).

Peer Review under the responsibility of Universidad Nacional Autónoma de México.

1. Introduction

Environmental problems associated with the textile industry are generally related with the contamination by the discharge of colored wastewater into water bodies. The presence of synthetic colorants significantly affects the well-being of the aquatic ecosystems since it significantly reduces the concentration of dissolved oxygen, they interact with light and, consequently, decreases the photosynthetic activity of many species (Khraisheh et al., 2005; Semião et al., 2020; Sheshdeh et al., 2014). In addition, the adverse effects of some of these dyes on human health have been reported due to their carcinogenic and mutagenic properties (Elsagh et al., 2017; Kittappa et al., 2020). But not only the effect of their discharges affects when they are discharged into bodies of water, but also the damages are observed when the colored effluents are deposited in the soil, deteriorating their quality as well as their fertility, accumulating pollutants with harmful effects for the living beings (Patel et al., 2020). Consequently, it is necessary to remove the colorants from the industrial effluents before they enter as final disposition to the water bodies.

Various technologies, including adsorption, flocculation, membrane separation, chemical oxidation, and photocatalytic degradation, among others, have been used to treat colored wastewater (Bilińska et al., 2019; Chen et al., 2020; Xia et al., 2020); among which adsorption is considered to be economically efficient and very favorable (Awasthi & Datta, 2019; Naushad et al., 2019), mainly for industrial treatments in fixed bed columns (Alardhi et al., 2020; Charola et al., 2018). For the elimination of colorants in solution different types of adsorbent materials have been studied, with good adsorption properties, which include the activated carbon (Castellar-Ortega et al., 2020; Daoud et al., 2019; Patra et al., 2020), carbon nanotubes (Dutta et al., 2018; Elsagh et al., 2017; Saxena et al., 2020); biomass (Cheruiyot et al., 2019; da Silva & Pietrobelli, 2019; Jia et al., 2017), clays (Bentahar et al., 2019; Jawad & Abdulhameed, 2020; Thirumoorthy & Krishna, 2020), chitosan (da Silva et al., 2020; Lipatova et al., 2018; Muedas-Taípe et al., 2020), bentonite (Khalilzadeh Shirazi et al., 2020; Saeed et al., 2020; Santos et al., 2020), zeolites (Abdelrahman, 2018; Humelnicu et al., 2017; Rashid et al., 2020) and diatomites (Mohamed et al., 2019; Sriram et al., 2020; Xia et al., 2020) among others.

Activated carbon is perhaps the most widely used in the removal of dyes, but its high cost directed the attention of research towards the study of cheap, effective, readily available and low cost materials; especially those natural solid materials with abundant reserves and easy access (Yan et al., 2018; Zhang et al., 2013). In this sense, diatomaceous earth or diatomite has been shown to be an alternative adsorbent to remove ions and colorants from wastewater (Caliskan et al.,

2011; Sheshdeh et al., 2014; Xia et al., 2020), thanks to its porous structure and large pore size distribution (Liu et al., 2019; Mu et al., 2018). It consists mainly of amorphous silica ($\text{SiO}_2 \cdot n\text{H}_2\text{O}$) (Šljivić et al., 2009), formed by remains of fossilized micro skeletons of diatoms, microscopic unicellular marine organisms related with the algae.

The objective of this research was to evaluate the adsorption capacity of diatomaceous earth from Chivata (Boyaca-Colombia), as an adsorbent material in the removal of crystal violet dye. The effect of temperature, pH and initial concentration was studied, keeping the adsorbent dose constant and the stirring. The experimental data were fitted to different models of adsorption isotherms.

2. Methodology

2.1. Source of diatomaceous earth

Diatomaceous earth samples come from the mine El Pino ($5^{\circ}34'15''$ north latitude and $73^{\circ}18'48''$ west longitude) of the municipality of Chivata, located at the central eastern region of the department of Boyaca – Colombia (Figure 1). The economy of the region is developed mainly in areas of commerce, manufacturing, agriculture and the construction sector with percentages of the 18.9%, 11.56%, 10.12% and 10.13% respectively; it should be noted that the mining and quarrying sector was accounted for a 8.11% (DNP, 2018). According the UPME (Unidad de Planeación Minero-Energética) in its report of 2019, this region exploits some materials such as ceramic, ferruginous and miscellaneous clays, and minerals such as coal (UPME, 2019).

2.2. Diatomaceous earth washing

Prior to washing the diatomaceous earth, a visual separation was made of those parts that presented a coloration different from their natural appearance, then it was crushed in a mortar (Figure 2) and passed through a sieve No. 50 ($300 \mu\text{m}$).

The sieved sample was washed with hot distilled water to remove fine material and other impurities. Finally, it was dried by 12 h to 105°C and reserved in a desiccator for later use (Šljivić et al., 2009).

2.3. Characterization of diatomaceous earth

The inorganic functional groups of diatomaceous earth before and after the removal of the crystal violet dye were analyzed by Fourier transform infrared spectrophotometry (FTIR), in the range between 4000 and 400 cm^{-1} by KBr pellet method on a spectrometer mark Nicolet iS 10 Thermo Fisher Scientific. The texture properties were determined from the adsorption-desorption isotherm of N_2 at 77 K in a sorptometer Micromeritics Gemini 2375. The morphology was evaluated by scanning electron microscopy (SEM) in a Vega3 Tescan SBU equipment. Lastly, the point of zero charge (PZC) was determined adding

50 cm³ of deionized water to 0.5 g of diatomaceous earth, adjusting the initial pH between 3 and 10 units, with dilute solutions of sodium hydroxide (NaOH) and hydrochloric acid (HCl). After 48 hours the final pH of the samples was measured.

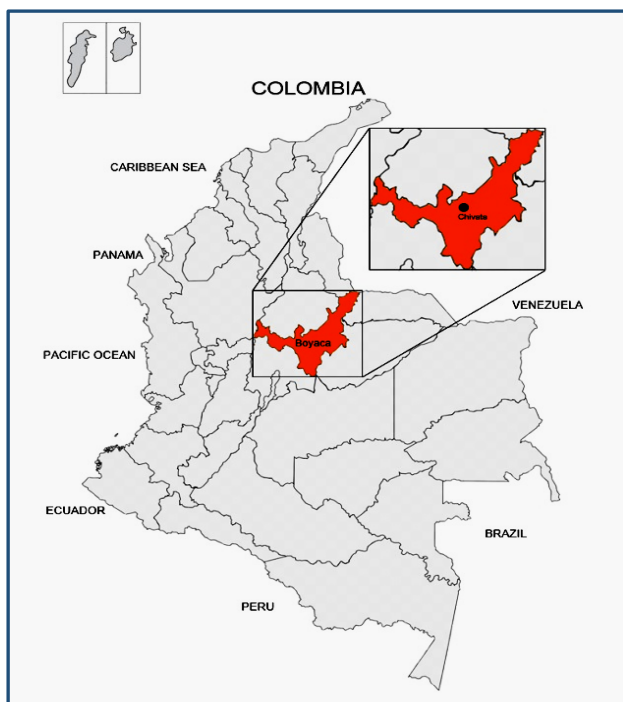


Figure 1. Map of Colombia. Diatomaceous earth deposit area, municipality of Chivata (Boyaca-Colombia).

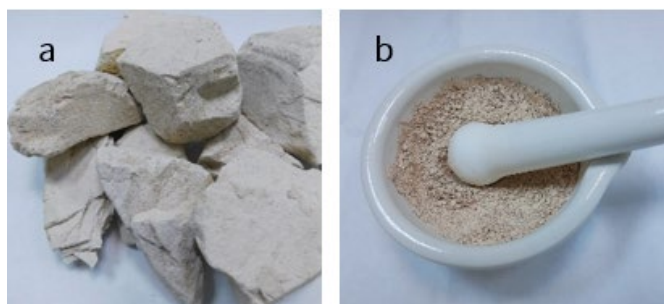


Figure 2. Diatomaceous earth: (a) initial sample and (b) crushed in mortar.

2.4. Adsorption study

Crystal violet is an organic, synthetic and alkaline dye with a molecular formula C₂₅H₃₀N₃Cl with molar molecular mass of 407.99 g/mol (Figure 3). For the construction of the calibration curve of the dye, 5 solutions were prepared between 1 and 5 mg/dm³ and the absorbance at 583 nm obtained by previous scanning was determined for each one, in a UV-Vis spectrophotometer mark Shimadzu UV-1800. To establish the calibration curve, 4 replications were performed for a total of 20 tests.

For the batch study, a "stock" solution of 1000 mg/dm³ of the crystal violet colorant, was prepared dissolving the required amount in distilled water. From this solution, dilutions were prepared at concentrations of 300 and 1000 mg/dm³, adjusting the pH between 5 and 8 units with HCl and NaOH diluted.

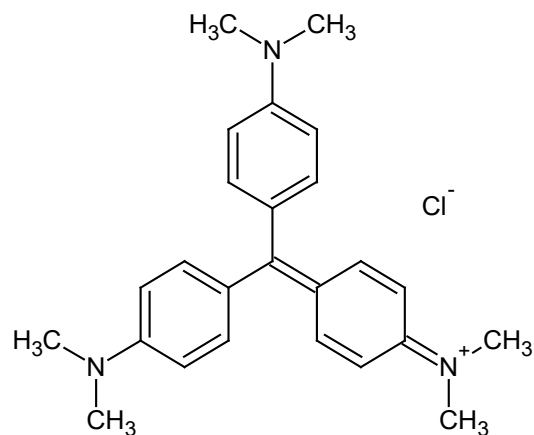


Figure 3. Molecular structure of crystal violet dye.

To 200 mg of diatomaceous earth were added 20 cm³ of each of the dilutions, then they were placed on a horizontal shaker at 120 rpm per 2 hours (estimated time to reach the equilibrium condition), in a thermostated bath. The temperatures selected for this work were 30, 35 and 40°C. Finally, the samples were filtered, an aliquot was taken, and the concentration was determined to 583 nm, in a spectrophotometer UV-Vis mark Shimadzu UV-1800.

The removal percentage and the adsorption capacity (*q*) of the diatomite were calculated from the Eqs. 1 and 2 respectively.

$$\% \text{ Removal} = \frac{C_o - C_e}{C_o} \times 100 \quad (1)$$

$$q = \frac{(C_o - C_e)V}{m} \quad (2)$$

Where *C_o* y *C_e* represent the initial and equilibrium concentration of the crystal violet dye respectively in mg/dm³, *V* is the volume of the solution used in dm³ and *m* is the mass of diatomaceous earth used in g.

In this research a categorical multifactorial design was developed, with factors such as the effect of the initial concentration of the dye (300, 400, 500, 600, 800 and 1000 mg/dm³), the temperature (30, 35 and 40°C) and the initial pH (5, 6, 7 and 8), and as a dependent variable the removal capacity of diatomaceous earth and the removal percentage of the crystal violet dye. 4 repetitions were carried out for a total of 288 tests.

3. Results

3.1. Characterization

The Figure 4 shows SEM micrograph of diatomaceous earth after washing. It is observed that most of the frustules have cylindrical geometry with different dimensions and well-developed porous structure clearly visible on their surface.

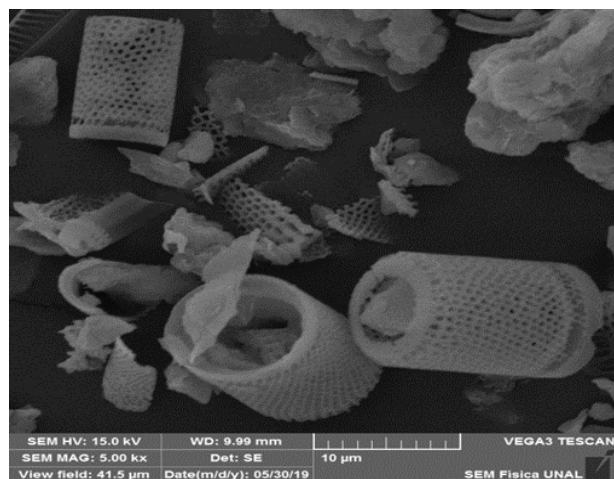


Figure 4. SEM micrograph of diatomaceous earth.

The Figure 5 shows the IR spectrum of diatomaceous earth. Different characteristic bands of the SiO₂ are observed that appear systematically in this type of materials and are mainly due to vibrations of the silicon-oxygen bond. The absorption band at frequencies between 1100 and 1000 cm⁻¹ corresponds to the asymmetric stretching vibration modes of the bond Si-O-Si (siloxane groups) (Khraisheh et al., 2005); the bands to 912 and 791 cm⁻¹ are due to Si-OH stretching of silanol groups and, the bending modes of Si-O-Si and O-Si-O to at 536 and 468 cm⁻¹ bonds, respectively (Sheshdeh et al., 2014). The bands in 3696 and 3620 cm⁻¹ are due to free silanol groups on the surface (Caliskan et al., 2011; Khraisheh et al., 2005). Regarding the stretching vibrations of the hydroxyl groups, a broad band with low intensity at high frequency is observed close to 3400 cm⁻¹, which corresponds to the vibrational mode of the O-H bond of molecular water absorbed with hydrogen bonds; to 1652 cm⁻¹ due to the angular deformations of the water (H-O-H) and the band around of 990 cm⁻¹ assigned to the vibrations of Si-OH bonds.

In the Figure 5 also shown is the IR spectrum of diatomaceous earth after the dye adsorption process. The changes are not significant, but if it is observed that the two bands between the 3690 and 3620 cm⁻¹ they become less intense and softer, which suggests tension of N-H bonds resulting from the interaction between the amino groups of the dye with the silanol groups of the diatomite. Close to the 1590 cm⁻¹ a new band is observed possibly due to bending of the N-H bond.

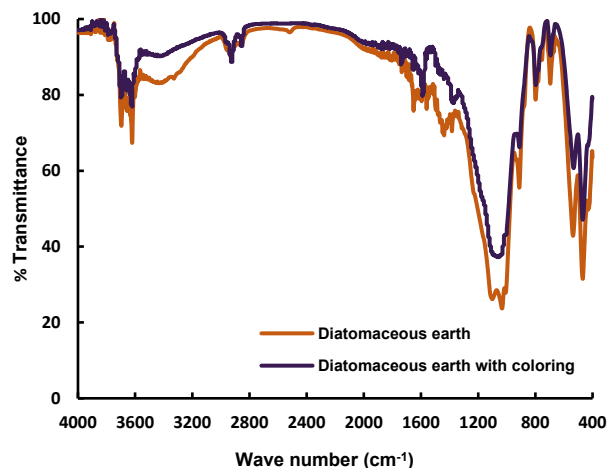


Figure 5. IR spectra of diatomaceous earth before and after adsorption of the crystal violet dye.

The point of zero charge (PZC) allows to determine the pH, at which the surface of the adsorbent material is neutral. This implies that those adsorbents with pH values higher than the PZC have a surface with a predominance of negative charges, while, at pH lower than the PZC will have a surface with a predominance of positive charges (Semião et al., 2020). In the Figure 6 the curve that results from graphing the pH of the solutions after 48 h and the initial pH line is observed, the intercept between the two shows that the point of zero charge for diatomaceous earth corresponds to pH 5. This result suggests that hydroxyl groups on the surface of diatomite (verified from the FTIR study) can gain or lose a proton by changing the pH.

This result suggests that hydroxyl groups on the surface of diatomite (verified from the FTIR study) can gain or lose a proton by changing the pH.

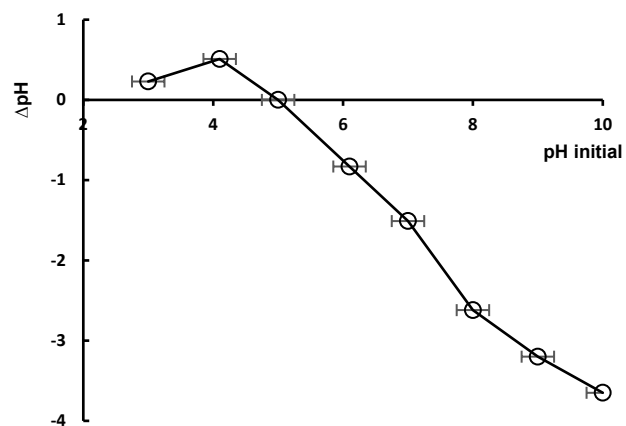
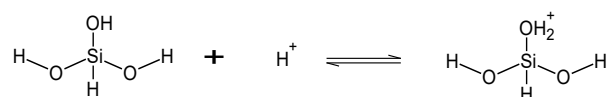
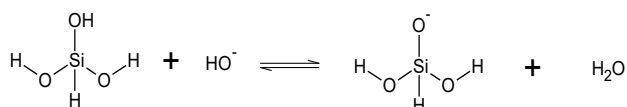


Figure 6. Point of zero charge of diatomaceous earth.

At pH values less than 5, the surface of the diatomite gains a proton and becomes positively charged according to the following scheme.



To pH equal to 5, both positive and negative charges are equal, but at pH above 5, the surface loses protons and becomes negatively charged as shown below.



The adsorption-desorption isotherms with N₂ at 77 K of diatomaceous earth is shown in Figure 7. According IUPAC classification corresponds to a Type IV (a) isotherm (Cychosz & Thommes, 2018), with closed hysteresis ring Type H3, which indicates the presence of mesopores. The specific area was calculated applying the Brunauer, Emmett and Teller method (BET) using the adsorption data in the range of relative pressures between 0.05 and 0.15; the pore size distribution was determined by the method of Barret, Joyner and Halenda (BJH) and the total pore volume was estimated from the amount of nitrogen adsorbed at the relative pressure of 0.99. The results are shown in Table 1.

The surface area of diatomaceous earth evaluated in this investigation is low (39.0 m²/g), compared with other adsorbent materials used in dye removal. Its external area of 35.6 m²/g very close to surface area, confirms that its pore structure is primarily mesoporous, as indicated by average pore size (5.83 nm). Under these circumstances, the role played by the surface chemistry of diatomaceous earth is significant and perhaps more relevant than the textural properties.

Table 1. Textural properties of diatomaceous earth.

Property	Value
Superficial area BET (m ² /g)	39.0
External area BET (m ² /g)	35.6
Pore volume BJH (cm ³ /g)	0.10
Average pore size BJH (nm)	5.83

3.2. Adsorption of crystal violet dye

3.2.1. Effect of initial pH

The Figure 8 shows the effect of initial pH on the adsorption capacity of diatomaceous earth at an initial concentration of 1000 mg/dm³ at all temperatures evaluated. It is observed that

as the pH increases the capacity increases, until reaching the highest experimental value of 94.5 mg/g at pH 8 and 30°C. For this same pH at temperatures of 35 and 40°C there is a slight decrease in the adsorption capacity of diatomaceous earth due to desorption processes at the surface.

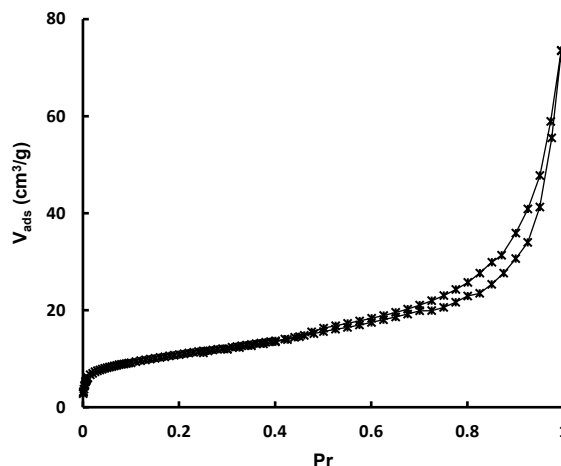


Figure 7. Adsorption-desorption isotherm with N₂ at 77 K of the diatomaceous earth.

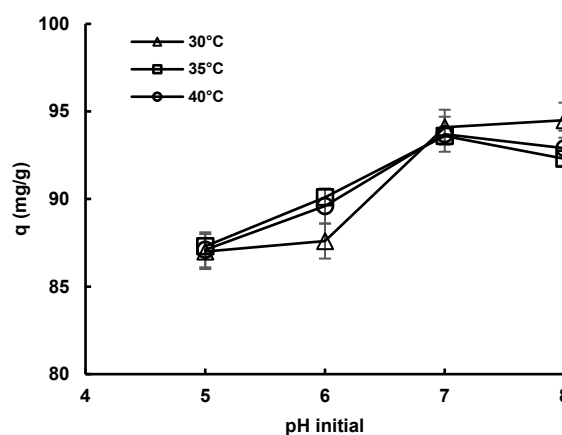


Figure 8. Effect of pH on the removal capacity at initial concentration of 1000 mg/dm³.

The point of zero charge showed that from pH 5 the surface of diatomaceous earth becomes negatively charged, which favors electrostatic attraction with the positively charged colorant, however, the presence of H⁺ ions at pH values below 7, which compete for active adsorption sites, decreases the capacity of diatomaceous earth.

3.2.2. Effect of initial concentration

In the Figure 9 the effect of the initial concentration of the crystal violet dye is shown in the range of 300 to 1000 mg/dm³ on the percentage of removal and the adsorption capacity of diatomaceous earth at 30°C at the evaluated pH values.

From the Figure 9a it is observed that the removal percentage decreases with the increase of the initial concentration. The above behavior is due to the greater availability of active adsorption sites in diatomaceous earth at low concentrations, therefore, all or a large part of the molecules of the crystal violet dye can be removed from the solution, reaching percentages close to 100% for all evaluated pH. As the initial concentration increases, more molecules of the dye compete for the available active sites and even after reaching equilibrium, molecules remain in the solution, reducing the percentage up to 87% to pH 5. Regarding the adsorption capacity, Figure 9b shows that it increases as the initial concentration increases. This is due to the fact that the driving force of adsorption processes is the difference in concentration of the dye present in the adsorbent and in solution; a low concentration gradient causes slow transport due to a decrease in the diffusion coefficient or mass transfer coefficient; while increasing the initial concentration causes a faster transport and, consequently, increases the adsorption capacity.

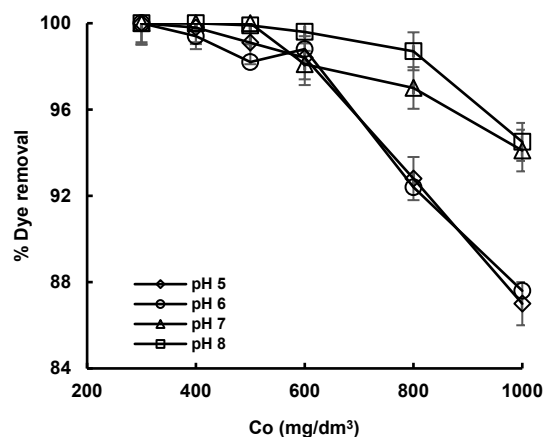
3.2.3. Effect of temperature

The Figure 10 shows the effect of temperature on the adsorption capacity of diatomaceous earth at the initial concentration of 1000 mg/dm³ at all evaluated pH. From the figure it can be seen that at pH 5, the variation in the adsorption capacity of diatomaceous earth is very low, so that it can be considered constant as the temperature varies; there is only a slight decrease when increasing the pH to 7 and 8. This little noticeable behavior is due to the fact that as the temperature increases, the diffusion speed of the dye molecules in the internal pores of the adsorbent increases so much (Sheshdeh et al., 2014), as the vibrational energy of the adsorbed molecules. Consequently, they desorb from the surface, decreasing the capacity of diatomaceous earth.

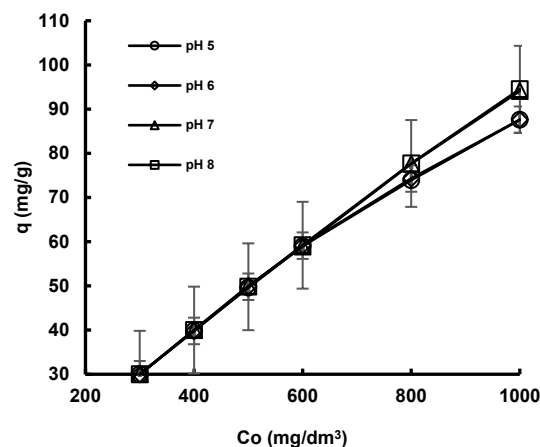
3.2.4. Adsorption isotherms

The Adsorption isotherms are used mainly to analyze the nature of the interaction between adsorbent and adsorbate and their relationship at equilibrium. In this research, the experimental results were adjusted to two models of adsorption isotherms: Langmuir and Freundlich. Langmuir's isotherm model assumes that adsorption occurs at identical active sites on the adsorbent surface, restricting itself to monolayer coverage; that is, once the dye molecule occupies a place on the surface of the diatomaceous earth, no further adsorption can occur at this same site and there is no

interaction between the adsorbed molecules (Castellar-Ortega et al., 2020; Vithalkar & Jugade, 2020). Equation 3 represents the linear form of the model.



(a)



(b)

Figure 9. Effect of the initial concentration on a) the percentage of removal and b) the removal capacity of diatomaceous earth at 30°C.

$$\frac{C_e}{q_e} = \frac{C_e}{q_{max}} + \frac{1}{K_L q_{max}} \quad (3)$$

Where C_e is the equilibrium concentration of the crystal violet dye in mg/dm³, q_e is the equilibrium adsorption capacity in mg/g, q_{max} is the maximum adsorption capacity in mg/g and K_L is the Langmuir constant in dm³/mg. The values of K_L and q_{max} were calculated from the slope and the intercept when graphing C_e/q_e versus C_e . Freundlich isotherm model assumes that the heat of adsorption is not constant, because it varies exponentially with the extent of the covered surface, a condition closer to reality than assumed by Langmuir. This assumption implies that the surface of the adsorbent is

heterogeneous and that the adsorption sites have different affinities (Semião et al., 2020). The equation 4 represents the linear form of the model.

$$\ln q_e = \frac{1}{n} \ln C_e + \ln K_F \quad (4)$$

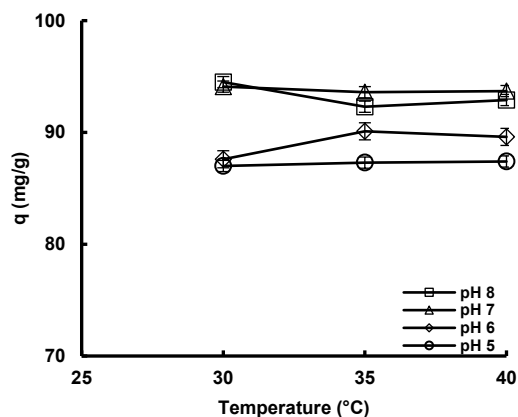


Figure 10. Effect of temperature on the adsorption capacity of diatomaceous earth at the initial concentration of 1000 mg/L.

Where K_F is Freundlich constant and n is a constant related to the affinity between the adsorbent and the solute. Table 2 shows the values of the constants of both models.

For all the process conditions evaluated in this study, the experimental data fit the Langmuir isotherm model very well, with a correlation factor between 0.97 and 0.99. Therefore, it can be inferred that the adsorption process occurred on a homogeneous surface with monolayer formation. The maximum adsorption capacity of diatomaceous earth was of 96.1 mg/g to pH 8 and 30°C (Table 2), slightly higher than the experimental value of 94.5 mg/g. The values of n obtained from the Freundlich model are greater than 1, which indicates that the adsorption is favorable for all the conditions studied.

The characterization of the diatomaceous earth and the results of the adsorption isotherms indicate that the removal may be due in the first place, to the electrostatic attractive force between the surface of the negatively charged adsorbent at pH above 5 and, the positively charged violet crystal dye and, secondly, the presence of silanol groups that extend on the surface of the silica, which allow hydrogen bonds to be established with the nitrogen atoms of the violet crystal. A diagram of these interactions is shown in Figure 11.

It is important to note that diatomaceous earth, under the conditions studied in this research, shows a greater adsorption capacity than other traditional and alternative adsorbents (Table 3), which allows it to be included within the materials with potential for practical applications in the treatment of colored wastewater.

Table 2. Langmuir and Freundlich isotherms constants.

Temperature (°C)	pH	Langmuir isotherm			Freundlich isotherm		
		q_{max} (mg/g)	K_L (dm ³ /mg)	R^2	K_F	n	R^2
30	5	87.7	0.20	0.99	39.9	6.4	0.99
	6	90.1	0.17	0.99	35.1	5.3	0.95
	7	95.2	0.32	0.97	38.6	4.9	0.94
	8	96.1	0.30	0.99	42.3	5.2	0.97
35	5	89.3	0.23	0.99	44.8	8.2	0.91
	6	90.1	0.18	0.99	43.0	6.4	0.87
	7	94.3	0.42	0.98	35.1	4.2	0.99
	8	93.4	0.33	0.99	49.6	8.2	0.92
40	5	87.7	0.24	0.99	39.4	6.2	0.91
	6	91.7	0.20	0.99	37.4	5.4	0.96
	7	94.3	0.45	0.99	36.5	4.4	0.99
	8	93.4	0.37	0.99	47.5	6.9	0.93

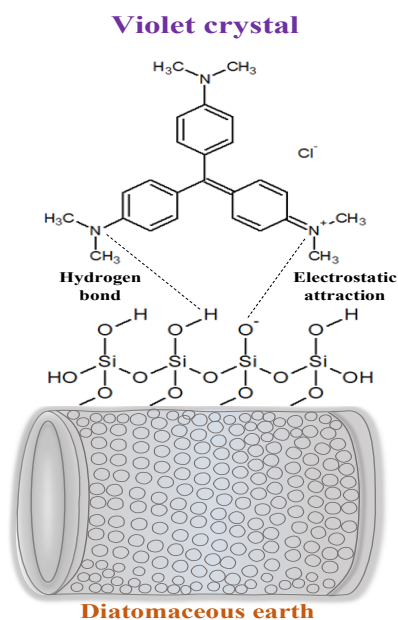


Figure 11. Diagram of the possible adsorption mechanism between diatomaceous earth and crystal violet. Adapted from Siram et al., 2020.

Table 3. Comparison of the maximum removal capacity of diatomaceous earth in this investigation with other adsorbent materials.

Adsorbent	Maximum adsorption capacity (mg/g)	Ref.
Activated carbon	85.84	(Senthilkumar et al., 2006)
Chitosan hidrogel beads	76.9	(Pal et al., 2013)
Silver nanoparticles immobilized on the activated carbon	87.2	(AbdEl-Salam et al., 2017)
Biopolymers composites with peanut hull	100.6	(Tahir et al., 2017)
Activated carbon	50.1	(Yakout et al., 2019)
Chitosan-coated bentonite	169.5	(Vithalkar & Jugade, 2020)
This work	96.1	

3.3. Statistical analysis

For the statistical analysis a categorical multifactorial design was developed, which was based on an analysis of variance of factors such as the initial concentration of the dye, temperature and the initial pH of the solutions and, as a dependent variable, the removal percentage of the crystal

violet dye. Several tests were performed to determine which factors had a statistically significant effect on the percentage of removal.

The Table 4 shows the ANOVA analysis, where the variability of the removal percentage (response variable) is decomposed into contributions due to the different study factors. The Type III sum of squares (by default) was selected, where the contribution of each factor is measured by eliminating the effects of the other factors. The P-values test the statistical significance of each of the factors. Since 4 P-values are less than 0.05, these factors have a statistically significant effect on removal with 95.0% of confidence level. According to the above, the initial pH and concentration factors have a significant effect at the different levels, as are their interactions. From this analysis and using the multiple range test, the estimated differences of the means were analyzed. The method used to discriminate between means is Fisher's least significant difference (LSD) procedure; with this method there is a risk of 5.0% at saying that each pair of means is significantly different, when the real difference is equal to 0.

4. Conclusions

In this research, diatomaceous earth from the municipality of Chivata (Boyaca-Colombia) was used to remove the crystal violet dye in solution. Its physicochemical characterization shows the presence of cylindrical frustules with development of porosity, but low surface area, with mainly silanol and silane groups on their surface. From the statistical analysis it is observed that the effect of pH and the initial concentration of the dye on the adsorption capacity and removal percentage of diatomaceous earth is greater than the effect of temperature, which is not significant. The percentage of removal of the violet crystal by diatomaceous earth increases as the concentration of the treated solution decreases and the removal capacity of the diatomaceous earth increases as the concentration and initial pH of the treated solution increase. The experimental results show a good fit to the Langmuir isotherm model with correlation factors close to 0.99, which indicates a homogeneous surface with mainly monolayer coverage. The maximum adsorption capacity of the crystal violet dye was of 96.1 mg/g at pH 8 and 30°C, which makes it an attractive adsorbent material for the removal of colorants in wastewater, considering that it was used without any type of modification.

Table 4. Analysis of variance for removal - Sum of Squares Type III.

Source	Sum of squares	Gl	Medium square	Reason-F*	Value-P
MAIN EFFECTS					
A: concentration	2174.02	4	543.506	2071.75	0.0000
B: temperature	0.403698	2	0.201849	0.77	0.4652
C: pH	172.124	3	57.3747	218.70	0.0000
INTERACTIONS					
AB	1.0271	8	0.128387	0.49	0.8623
AC	206.741	12	17.2285	65.67	0.0000
BC	14.0332	6	2.33886	8.92	0.0000
RESIDUE	37.7771	144	0.262341		
TOTAL (CORRECTED)	2606.13	179			

* All F-ratios are based on the mean square of the residual error.

Conflict of interest

The authors do not have any type of conflict of interest to declare.

Acknowledgments

The authors of this article are grateful for the collaboration of the Laboratorio de Química of the Universidad Autónoma del Caribe, the Laboratorio de Combustibles y Energía of the Universidad Nacional de Colombia, and the Laboratorio de Biotecnología de Microalgas of the Universidad del Atlántico.

Financing

The authors received no specific funding for this work.

References

Abdel-Salam, A. H., Ewais, H. A., & Basaleh, A. S. (2017). Silver nanoparticles immobilised on the activated carbon as efficient adsorbent for removal of crystal violet dye from aqueous solutions. A kinetic study. *Journal of Molecular Liquids*, 248, 833–841.
<https://doi.org/10.1016/j.molliq.2017.10.109>

Abdelrahman, E. A. (2018). Synthesis of zeolite nanostructures from waste aluminum cans for efficient removal of malachite green dye from aqueous media. *Journal of Molecular Liquids*, 253, 72–82.
<https://doi.org/10.1016/j.molliq.2018.01.038>

Alardhi, S. M., Albayati, T. M., & Alrubaye, J. M. (2020). Adsorption of the methyl green dye pollutant from aqueous solution using mesoporous materials MCM-41 in a fixed-bed column. *Heliyon*, 6(1), e03253.
<https://doi.org/10.1016/j.heliyon.2020.e03253>

Awasthi, A., & Datta, D. (2019). Application of Amberlite XAD-7HP resin impregnated with Aliquat 336 for the removal of Reactive Blue - 13 dye: Batch and fixed-bed column studies. *Journal of Environmental Chemical Engineering*, 7(6), 103502.
<https://doi.org/10.1016/j.jece.2019.103502>

Bentahar, Y., Draoui, K., Hurel, C., Ajouyed, O., Khairoun, S., & Marmier, N. (2019). Physico-chemical characterization and valorization of swelling and non-swelling Moroccan clays in basic dye removal from aqueous solutions. *Journal of African Earth Sciences*, 154, 80–88.
<https://doi.org/10.1016/j.jafrearsci.2019.03.017>

Bilińska, L., Blus, K., Gmurek, M., & Ledakowicz, S. (2019). Coupling of electrocoagulation and ozone treatment for textile wastewater reuse. *Chemical Engineering Journal*, 358, 992–1001.
<https://doi.org/10.1016/j.cej.2018.10.093>

Caliskan, N., Kul, A. R., Alkan, S., Sogut, E. G., & Alacabey, I. (2011). Adsorption of Zinc(II) on diatomite and manganese-oxide-modified diatomite: A kinetic and equilibrium study. *Journal of Hazardous Materials*, 193, 27–36.
<https://doi.org/10.1016/j.jhazmat.2011.06.058>

Castellar-Ortega, G. C., Cely-Bautista, M. M., Cardozo-Arrieta, B. M., Angulo-Mercado, E. R., de Jesús Mendoza-Colina, E., Zambrano-Arevalo, A. M., Jaramillo-Colpas, J. E., & Rosales-Díaz, C. L. (2020). Removal of the direct navy-blue dye on modified coffee bean. *Tecnología y Ciencias del Agua*, 11(4), 1–26.
<https://doi.org/10.24850/j-tyca-2020-04-01>

- Charola, S., Yadav, R., Das, P., & Maiti, S. (2018). Fixed-bed adsorption of Reactive Orange 84 dye onto activated carbon prepared from empty cotton flower agro-waste. *Sustainable Environment Research*, 28(6), 298–308. <https://doi.org/10.1016/j.serj.2018.09.003>
- Chen, B., Long, F., Chen, S., Cao, Y., & Pan, X. (2020). Magnetic chitosan biopolymer as a versatile adsorbent for simultaneous and synergistic removal of different sorts of dyestuffs from simulated wastewater. *Chemical Engineering Journal*, 385, 123926. <https://doi.org/10.1016/j.cej.2019.123926>
- Cheruiyot, G. K., Wanyonyi, W. C., Kiplimo, J. J., & Maina, E. N. (2019). Adsorption of toxic crystal violet dye using coffee husks: Equilibrium, kinetics and thermodynamics study. *Scientific African*, 5, 1–11. <https://doi.org/10.1016/j.sciaf.2019.e00116>
- Cychosz, K. A., & Thommes, M. (2018). Progress in the Physisorption Characterization of Nanoporous Gas Storage Materials. *Engineering*, 4(4), 559–566. <https://doi.org/10.1016/j.eng.2018.06.001>
- da Silva, D. C. C., & Pietrobelli, J. M. T. D. A. (2019). Residual biomass of chia seeds (*Salvia hispanica*) oil extraction as low cost and eco-friendly biosorbent for effective reactive yellow B2R textile dye removal: Characterization, kinetic, thermodynamic and isotherm studies. *Journal of Environmental Chemical Engineering*, 7(2), 103008. <https://doi.org/10.1016/j.jece.2019.103008>
- da Silva, P. M. M., Comparotto, N. G., Lira, K. T. G., Picone, C. S. F., & Prediger, P. (2020). Adsorptive removal of basic dye onto sustainable chitosan beads: Equilibrium, kinetics, stability, continuous-mode adsorption and mechanism. *Sustainable Chemistry and Pharmacy*, 18, 100318. <https://doi.org/10.1016/j.scp.2020.100318>
- Daoud, M., Benturki, O., Girods, P., Donnot, A., & Fontana, S. (2019). Adsorption ability of activated carbons from *Phoenix dactylifera* rachis and *Ziziphus jujube* stones for the removal of commercial dye and the treatment of dyestuff wastewater. *Microchemical Journal*, 148(January), 493–502. <https://doi.org/10.1016/j.microc.2019.05.022>
- Dutta, A. K., Ghorai, U. K., Chattopadhyay, K. K., & Banerjee, D. (2018). Removal of textile dyes by carbon nanotubes: A comparison between adsorption and UV assisted photocatalysis. *Physica E: Low-Dimensional Systems and Nanostructures*, 99, 6–15. <https://doi.org/10.1016/j.physe.2018.01.008>
- Elsagh, A., Moradi, O., Fakhri, A., Najafi, F., Alizadeh, R., & Haddadi, V. (2017). Evaluation of the potential cationic dye removal using adsorption by graphene and carbon nanotubes as adsorbents surfaces. *Arabian Journal of Chemistry*, 10, S2862–S2869. <https://doi.org/10.1016/j.arabjc.2013.11.013>
- Humelnicu, I., Băiceanu, A., Ignat, M. E., & Dulman, V. (2017). The removal of Basic Blue 41 textile dye from aqueous solution by adsorption onto natural zeolitic tuff: Kinetics and thermodynamics. *Process Safety and Environmental Protection*, 105, 274–287. <https://doi.org/10.1016/j.psep.2016.11.016>
- Jawad, A. H., & Abdulhameed, A. S. (2020). Mesoporous Iraqi red kaolin clay as an efficient adsorbent for methylene blue dye: Adsorption kinetic, isotherm and mechanism study. *Surfaces and Interfaces*, 18, 100422. <https://doi.org/10.1016/j.surfin.2019.100422>
- Jia, Z., Li, Z., Ni, T., & Li, S. (2017). Adsorption of low-cost absorption materials based on biomass (*Cortaderia selloana* flower spikes) for dye removal: Kinetics, isotherms and thermodynamic studies. *Journal of Molecular Liquids*, 229, 285–292. <https://doi.org/10.1016/j.molliq.2016.12.059>
- Khalilzadeh Shirazi, E., Metzger, J. W., Fischer, K., & Hassani, A. H. (2020). Removal of textile dyes from single and binary component systems by Persian bentonite and a mixed adsorbent of bentonite/charred dolomite. *Colloids and Surfaces A: Physicochemical and Engineering Aspects*, 598, 124807. <https://doi.org/10.1016/j.colsurfa.2020.124807>
- Khraisheh, M. A. M., Al-Ghouti, M. A., Allen, S. J., & Ahmad, M. N. (2005). Effect of OH and silanol groups in the removal of dyes from aqueous solution using diatomite. *Water Research*, 39(5), 922–932. <https://doi.org/10.1016/j.watres.2004.12.008>
- Kittappa, S., Jais, F. M., Ramalingam, M., & Ibrahim, S. (2020). Functionalized magnetic mesoporous palm shell activated carbon for enhanced removal of azo dyes. *Journal of Environmental Chemical Engineering*, 8(5), 104081. <https://doi.org/10.1016/j.jece.2020.104081>
- Lipatova, I. M., Makarova, L. I., & Yusova, A. A. (2018). Adsorption removal of anionic dyes from aqueous solutions by chitosan nanoparticles deposited on the fibrous carrier. *Chemosphere*, 212, 1155–1162. <https://doi.org/10.1016/j.chemosphere.2018.08.158>

- Liu, H., Zhao, Y., Zhou, Y., Chang, L., & Zhang, J. (2019). Removal of gaseous elemental mercury by modified diatomite. *Science of the Total Environment*, 652, 651–659.
<https://doi.org/10.1016/j.scitotenv.2018.10.291>
- Mohamed, E. A., Selim, A. Q., Zayed, A. M., Komarneni, S., Mobarak, M., & Seliem, M. K. (2019). Enhancing adsorption capacity of Egyptian diatomaceous earth by thermo-chemical purification: Methylene blue uptake. *Journal of Colloid and Interface Science*, 534, 408–419.
<https://doi.org/10.1016/j.jcis.2018.09.024>
- Mu, Y., Cui, M., Zhang, S., Zhao, J., Meng, C., & Sun, Q. (2018). Comparison study between a series of new type functional diatomite on methane adsorption performance. *Microporous and Mesoporous Materials*, 267, 203–211.
<https://doi.org/10.1016/j.micromeso.2018.03.037>
- Muedas-Taípe, G., Mejía, I. M. M., Santillán, F. A., Velásquez, C. J., & Ascencios, Y. J. (2020). Removal of azo dyes in aqueous solutions using magnetized and chemically modified chitosan beads. *Materials Chemistry and Physics*, 256, 123595.
<https://doi.org/10.1016/j.matchemphys.2020.123595>
- Naushad, M., Alqadami, A. A., AlOthman, Z. A., Alsohaimi, I. H., Algamdi, M. S., & Aldawsari, A. M. (2019). Adsorption kinetics, isotherm and reusability studies for the removal of cationic dye from aqueous medium using arginine modified activated carbon. *Journal of Molecular Liquids*, 293, 111442.
<https://doi.org/10.1016/j.molliq.2019.111442>
- Pal, A., Pan, S., & Saha, S. (2013). Synergistically improved adsorption of anionic surfactant and crystal violet on chitosan hydrogel beads. *Chemical Engineering Journal*, 217, 426–434.
<https://doi.org/10.1016/j.cej.2012.11.120>
- Patel, V. R., Khan, R., & Bhatt, N. (2020). Cost-effective in-situ remediation technologies for complete mineralization of dyes contaminated soils. *Chemosphere*, 243, 125253.
<https://doi.org/10.1016/j.chemosphere.2019.125253>
- Patra, C., Gupta, R., Bedadeep, D., & Narayanasamy, S. (2020). Surface treated acid-activated carbon for adsorption of anionic azo dyes from single and binary adsorptive systems: A detail insight. *Environmental Pollution*, 266, 115102.
<https://doi.org/10.1016/j.envpol.2020.115102>
- Rashid, T., Iqbal, D., Hazafa, A., Hussain, S., Sher, F., & Sher, F. (2020). Formulation of zeolite supported nano-metallic catalyst and applications in textile effluent treatment. *Journal of Environmental Chemical Engineering*, 8(4), 104023.
<https://doi.org/10.1016/j.jece.2020.104023>
- Saeed, M., Munir, M., Nafees, M., Shah, S. S. A., Ullah, H., & Waseem, A. (2020). Synthesis, characterization and applications of silylation based grafted bentonites for the removal of Sudan dyes: Isothermal, kinetic and thermodynamic studies. *Microporous and Mesoporous Materials*, 291, 109697.
<https://doi.org/10.1016/j.micromeso.2019.109697>
- Santos, S. S. G., França, D. B., Castellano, L. R. C., Trigueiro, P., Silva Filho, E. C., Santos, I. M. G., & Fonseca, M. G. (2020). Novel modified bentonites applied to the removal of an anionic azo-dye from aqueous solution. *Colloids and Surfaces A: Physicochemical and Engineering Aspects*, 585, 124152.
<https://doi.org/10.1016/j.colsurfa.2019.124152>
- Saxena, M., Sharma, N., & Saxena, R. (2020). Highly efficient and rapid removal of a toxic dye: Adsorption kinetics, isotherm, and mechanism studies on functionalized multiwalled carbon nanotubes. *Surfaces and Interfaces*, 21, 100639.
<https://doi.org/10.1016/j.surfin.2020.100639>
- Semião, M. A., Haminiuk, C. W. I., & Maciel, G. M. (2020). Residual diatomaceous earth as a potential and cost effective biosorbent of the azo textile dye Reactive Blue 160. *Journal of Environmental Chemical Engineering*, 8(1), 103617.
<https://doi.org/10.1016/j.jece.2019.103617>
- Senthilkumaar, S., Kalaamani, P., & Subburaam, C. V. (2006). Liquid phase adsorption of crystal violet onto activated carbons derived from male flowers of coconut tree. *Journal of Hazardous Materials*, 136(3), 800–808.
<https://doi.org/10.1016/j.jhazmat.2006.01.045>
- Sheshdeh, R. K., Nikou, M. R. K., Badii, K., Limaee, N. Y., & Golkarnarenji, G. (2014). Equilibrium and kinetics studies for the adsorption of Basic Red 46 on nickel oxide nanoparticles-modified diatomite in aqueous solutions. *Journal of the Taiwan Institute of Chemical Engineers*, 45(4), 1792–1802.
<https://doi.org/10.1016/j.jtice.2014.02.020>
- Šljivić, M., Smičiklas, I., Pejanović, S., & Plečaš, I. (2009). Comparative study of Cu²⁺ adsorption on a zeolite, a clay and a diatomite from Serbia. *Applied Clay Science*, 43(1), 33–40.
<https://doi.org/10.1016/j.clay.2008.07.009>
- Sriram, G., Kigga, M., Uthappa, U. T., Rego, R. M., Thendral, V., Kumeria, T., Jung, H. Y., & Kurkuri, M. D. (2020). Naturally available diatomite and their surface modification for the removal of hazardous dye and metal ions: A review. *Advances in Colloid and Interface Science*, 282, 102198.
<https://doi.org/10.1016/j.cis.2020.102198>

Tahir, N., Bhatti, H. N., Iqbal, M., & Noreen, S. (2017). Biopolymers composites with peanut hull waste biomass and application for Crystal Violet adsorption. *International Journal of Biological Macromolecules*, 94, 210–220.

<https://doi.org/10.1016/j.ijbiomac.2016.10.013>

Thirumoorthy, K., & Krishna, S. K. (2020). Removal of cationic and anionic dyes from aqueous phase by Ball clay - Manganese dioxide nanocomposites. *Journal of Environmental Chemical Engineering*, 8(1), 103582.

<https://doi.org/10.1016/j.jece.2019.103582>

Vithalkar, S. H., & Jugade, R. M. (2020). Adsorptive removal of crystal violet from aqueous solution by cross-linked chitosan coated bentonite. *Materials Today: Proceedings*, 29, 1025–1032.

<https://doi.org/10.1016/j.matpr.2020.04.705>

Xia, K., Liu, X., Chen, Z., Fang, L., Du, H., & Zhang, X. (2020). Efficient and sustainable treatment of anionic dye wastewaters using porous cationic diatomite. *Journal of the Taiwan Institute of Chemical Engineers*, 000, 1–8.

<https://doi.org/10.1016/j.jtice.2020.07.020>

Yakout, S. M., Hassan, M. R., Abdeltawab, A. A., & Aly, M. I. (2019). Sono-sorption efficiencies and equilibrium removal of triphenylmethane (crystal violet) dye from aqueous solution by activated charcoal. *Journal of Cleaner Production*, 234, 124–131.

<https://doi.org/10.1016/j.jclepro.2019.06.164>

Yan, S., Huo, W., Yang, J., Zhang, X., Wang, Q., Wang, L., Pan, Y., & Huang, Y. (2018). Green synthesis and influence of calcined temperature on the formation of novel porous diatomite microspheres for efficient adsorption of dyes. *Powder Technology*, 329, 260–269.

<https://doi.org/10.1016/j.powtec.2018.01.090>

Zhang, J., Ping, Q., Niu, M., Shi, H., & Li, N. (2013). Kinetics and equilibrium studies from the methylene blue adsorption on diatomite treated with sodium hydroxide. *Applied Clay Science*, 83–84, 12–16.

<https://doi.org/10.1016/j.clay.2013.08.008>

UPME, Unidad de Planeación Minero Energética (2019). *Ministerio de Minas y Energía*.

<https://www1.upme.gov.co/simco/Cifras-Sectoriales/Paginas/arcillas.aspx>